Sustained H_2 Production Driven by Photosynthetic Water Splitting in a Unicellular Cyanobacterium

Matthew R. Melnicki, Grigoriy E. Pinchuk, Eric A. Hill, Leo A. Kucek, Jim K. Fredrickson, Allan Konopka, and Alexander S. Beliaev

Biological Sciences Division, Pacific Northwest National Laboratory, Richland, Washington, USA

ABSTRACT **The relationship between dinitrogenase-driven H_2 production and oxygenic photosynthesis was investigated in a unicellular cyanobacterium, *Cyanothece* sp. ATCC 51142, using a novel custom-built photobioreactor equipped with advanced process control. Continuously illuminated nitrogen-deprived cells evolved H_2 at rates up to 400 μmol · mg Chl^{-1} · h^{-1} in parallel with uninterrupted photosynthetic O_2 production. Notably, sustained coproduction of H_2 and O_2 occurred over 100 h in the presence of CO_2, with both gases displaying inverse oscillations which eventually dampened toward stable rates of 125 and 90 μmol · mg Chl^{-1} · h^{-1}, respectively. Oscillations were not observed when CO_2 was omitted, and instead H_2 and O_2 evolution rates were positively correlated. The sustainability of the process was further supported by stable chlorophyll content, maintenance of baseline protein and carbohydrate levels, and an enhanced capacity for linear electron transport as measured by chlorophyll fluorescence throughout the experiment. *In situ* light saturation analyses of H_2 production displayed a strong dose dependence and lack of O_2 inhibition. Inactivation of photosystem II had substantial long-term effects but did not affect short-term H_2 production, indicating that the process is also supported by photosystem I activity and oxidation of endogenous glycogen. However, mass balance calculations suggest that carbohydrate consumption in the light may, at best, account for no more than 50% of the reductant required for the corresponding H_2 production over that period. Collectively, our results demonstrate that uninterrupted H_2 production in unicellular cyanobacteria can be fueled by water photolysis without the detrimental effects of O_2 and have important implications for sustainable production of biofuels.**

IMPORTANCE **The study provides an important insight into the photophysiology of light-driven H_2 production by the nitrogen-fixing cyanobacterium *Cyanothece* sp. strain ATCC 51142. This work is also of significance for biotechnology, supporting the feasibility of "direct biophotolysis." The sustainability of the process, highlighted by prolonged gas evolution with no clear sign of significant decay or apparent photodamage, provides a foundation for the future development of an effective, renewable, and economically efficient bio-H_2 production process.**

Received 28 June 2012 **Accepted** 12 July 2012 **Published** 7 August 2012

Citation Melnicki MR, et al. 2012. Sustained H_2 production driven by photosynthetic water splitting in a unicellular cyanobacterium. mBio 3(4):e00197-12. doi:10.1128/mBio.00197-12.

Editor Roberto Kolter, Harvard Medical School

Address correspondence to Alexander S. Beliaev, alex.beliaev@pnnl.gov, and Allan Konopka, allan.konopka@pnnl.gov.

As the societal demand for fuel and energy continues to grow, much attention has been paid to H_2 as a renewable fuel. In addition to being a carbon-neutral molecule, H_2 can be enzymatically produced by microorganisms, thus facilitating the design of a production process with an environmentally friendly life cycle (1). Cyanobacteria and green algae are of particular interest because the products of light-catalyzed H_2O oxidation include the very substrates for H_2 production (2, 3). However, the integration of these two processes, sometimes described technologically as "direct biophotolysis," presents a serious paradox: O_2 is a byproduct of H_2O oxidation by photosystem II (PSII) and yet is a potent inhibitor of hydrogenase enzymes (4). Certain unicellular green algae, e.g., *Chlamydomonas reinhardtii*, and cyanobacteria, e.g., *Synechocystis* sp. PCC 6803, evolve H_2 under photosynthetic conditions using bidirectional hydrogenases as the terminal proton reductase to alleviate photoinhibition and/or equilibrate ATP insufficiencies during metabolic bottlenecks (5, 6). However, this occurs either transiently or during nutrient stresses whereby rates of H_2O photolysis fall below those of respiration, with the consequences of establishing anaerobiosis but also decreasing productivity (7).

A different opportunity is presented by N_2-fixing cyanobacteria, because dinitrogenase can serve as a strict hydrogenase in the absence of N_2 (8). This enzyme is also O_2 sensitive, but its unique role as the only biological input of N to the biosphere has driven cyanobacteria to develop strategies to cope with the O_2 paradox (9). A physical separation of photosynthesis and dinitrogenase is observed in heterocystous filamentous cyanobacteria, e.g., *Nostoc* and *Anabaena*, whereby vegetative cells fix CO_2 using linear electron transport and translocate organic carbon intermediates to differentiated heterocysts with downregulated PSII (10). Other strategies, involving temporal and spatial separation of the two processes within an individual cell, contribute to the majority of N_2 fixation in the ocean (11). Particularly, nonheterocystous filamentous cyanobacteria, e.g., *Trichodesmium*, carry out N_2 fixation only during the day in a fraction of cells, with the dinitrogenase

activity in these cells protected by a coordinated downregulation of PSII activity and high O_2 consumption rates (12). Unicellular diazotrophic cyanobacteria, e.g., *Cyanothece* and *Crocosphaera*, carry out N_2 fixation at night at the expense of stored photosynthate, which has accumulated during the day (13, 14).

The ability to spatially and temporally separate photosynthetic and dinitrogenase activities provides a foundation to exploit N_2-fixing cyanobacteria for H_2 production (15-17). Recent studies of *Cyanothece* sp. ATCC 51142 (here referred to as *Cyanothece* 51142) demonstrated that diazotrophically grown cultures entrained on light-dark cycles are capable of H_2 evolution under constant illumination during the "subjective dark" (18). The process was shown to be driven by dinitrogenase and was thought to rely upon respiration-induced microoxic environments resulting from oxidation of endogenous glycogen. While substantial H_2 production was shown to occur in the light, no mechanistic details linking photosynthetic metabolism and H_2 production in *Cyanothece* 51142 are available. To gain insight into the photophysiology of the process, we utilized a novel custom-built photobioreactor that coupled online gas monitoring and feedback-controlled lighting. To avoid circadian regulation (19), continuous illumination was used to grow low-density cultures in an N-limited chemostat where H_2 production was achieved by interrupting the influx of NH_4^+. The ability to monitor and control gas and light input into the system afforded high-resolution physiological details, opening a window on the relationship between photosynthetic O_2 evolution and H_2 production in unicellular cyanobacteria. Furthermore, the combination of nutrient-limited chemostat cultivation and feedback-controlled illumination enabled us to sustain long periods of light-driven H_2 production in *Cyanothece* 51142.

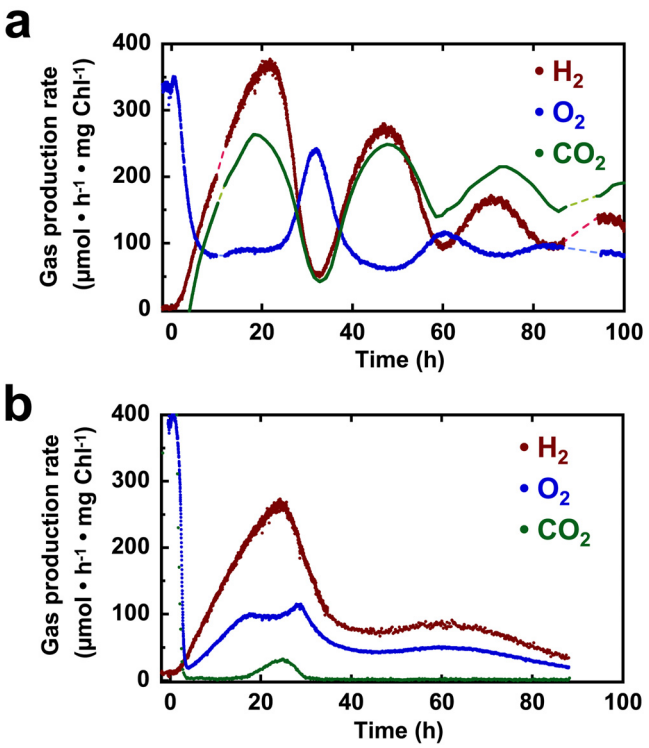

FIG 1 Gas dynamics by N-deprived *Cyanothece* 51142 cultures. Fine-scale resolution of production rate dynamics was obtained in the LED photobioreactor upon interruption of NH_4^+ influx, during continuous sparging with 1.3% CO_2-Ar (a) or pure Ar (b).

RESULTS

H_2 production under continuous light. When grown under continuous illumination, NH_4^+-limited chemostat cultures of *Cyanothece* 51142 express high levels of dinitrogenase (20), which is the primary catalyst of H_2 production in diazotrophic cyanobacteria (8). Under these steady-state conditions, *Cyanothece* 51142 evolved O_2 at a rate of 350 μmol · mg Chl^{-1} · h^{-1}; however, no H_2 was detected. Light-dependent H_2 production was observed only after chemostat-grown cells were transferred into sealed tubes and incubated under continuous light. Notably, after 72 h of continuous illumination with white light under an Ar atmosphere, *Cyanothece* 51142 cells evolved 4.46 ± 0.58 mmol H_2 · mg Chl^{-1} and 2.65 ± 0.14 mmol O_2 · mg Chl^{-1}, implying PSII activity as well as a possible O_2 tolerance (see Fig. S1 in the supplemental material). In order to observe the relationship between the H_2 and O_2 which had accumulated in sealed tubes, N deprivation was imposed directly on the chemostat culture by transitioning to batch mode via interruption of medium influx to the bioreactor. As a result, H_2 became detectable within 1 h upon the perturbation, and its production rates steadily accelerated to 400 μmol · mg Chl^{-1} · h^{-1} over the next 24-h period; at the same time, the rate of O_2 evolution began to gradually decline until it reached a stable level of ~100 μmol · mg Chl^{-1} · h^{-1} (Fig. 1a). Because of continuous sparging with Ar-CO_2 gas mix, the detection of O_2 and H_2 in the bioreactor indicated that both gases were continuously produced throughout the experiment. Nevertheless, after an initial phase of 24 h, oscillations commenced, whereby 12-h phases of increasing O_2 evolution alternated with phases of elevated H_2 and CO_2 production. These oscillations eventually dampened, exhibiting median H_2 and O_2 production rates of 125 and 90 μmol · mg Chl^{-1} · h^{-1} at the end of the experiment (100 h). Thus, not only did H_2 evolution occur simultaneously with oxygenic photosynthesis, these two processes proceeded concomitantly over a long, sustained period.

The effects of disrupting substrate flows were also investigated by additionally removing CO_2 from the sparge gas when halting the influx of NH_4^+ (Fig. 1b). Once again, H_2 became detectable shortly after N deprivation, with rates which also steadily increased over the first 24 h. As CO_2 levels in the off-gas quickly diminished, O_2 evolution rates also decreased rapidly, reaching values much lower than those found in the reactor sparged with Ar-CO_2. However, O_2 evolution rates began to recover at 4 h, remarkably increasing in parallel with H_2 evolution. From 17 to 28 h, however, O_2 evolution deviated from the H_2 dynamics, as a transient CO_2 evolution peak was detectable in the off gas. Upon the disappearance of CO_2, the O_2 resumed its mirroring of the H_2 dynamics, which had already begun to decelerate. Although the gas dynamics were dampened by 48 h, a second low-level oscillation of H_2 production occurred from 48 to 90 h, with a maximum at approximately 60 h, corresponding with small but discernible changes in the O_2 rate at these times. No CO_2 in the off-gas was detected throughout this second oscillation. Thus, under conditions where no external electron acceptors are available, phases of H_2 and O_2 evolution were positively correlated.

Macromolecular dynamics during photobiological H_2 production. Correlation between H_2 and CO_2 dynamics in the off-gas suggests that the catabolism of cellular carbon reserves may play a

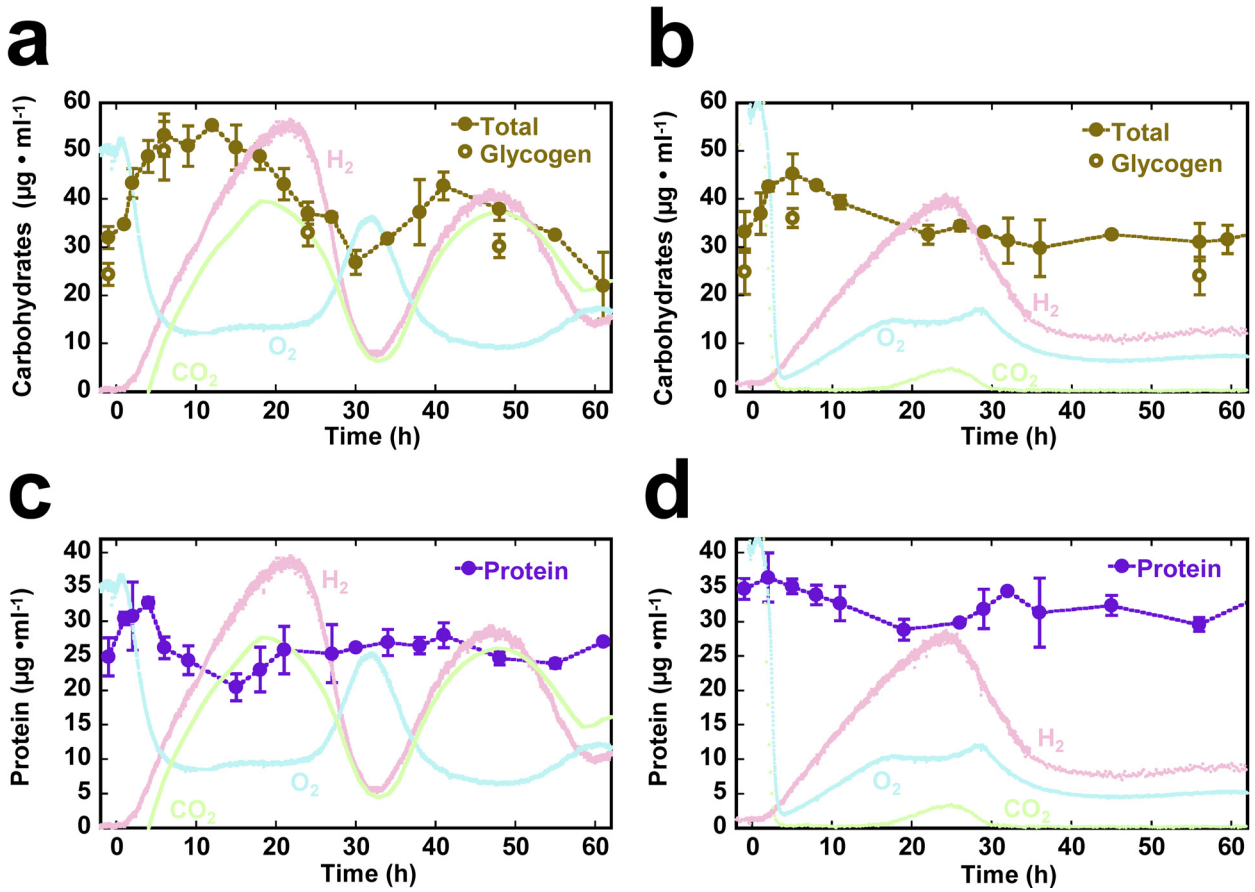

FIG 2 Carbohydrate (a, b) and protein dynamics (c, d) during H_2 production within the LED photobioreactor, during continuous sparging with 1.3% CO_2-Ar (a, c) or pure Ar (b, d). Carbohydrate measurements are based on glucose equivalents; open circles denote glycogen determination. Protein measurements are standardized to bovine serum albumin. Average values and standard deviations are based on at least two independently assayed sample replicates at each time point.

role in H_2 evolution by *Cyanothece* 51142. Within the first few hours after interrupting the NH_4^+ supply, the total carbohydrate levels in both reactors increased, reaching 55 mg · liter^{-1} in 12 h with Ar-CO_2 and 45 mg · liter^{-1} in 6 h with Ar (Fig. 2a and b). Thereafter, for both reactors, the carbohydrate content declined for the remainder of the first H_2 evolution cycle and well into the following phase of decelerating H_2 activity. Mass balance calculations for this time period indicate that the theoretical contribution of carbohydrate consumption may, at best, account for 40 and 51% of the electrons necessary for the corresponding H_2 production observed under Ar-only and Ar-CO_2 conditions, respectively (see Fig. S2a and b in the supplemental material). Furthermore, in the reactor sparged only with Ar, the total carbohydrate level remained relatively constant throughout the second half of the experiment, despite the H_2 production, which continued to proceed without interruption (see Fig. S2c in the supplemental material). However, in the Ar-CO_2 reactor, there was a second oscillation from 30 to 60 h, slightly offset from the H_2 dynamics, with carbohydrate accumulation occurring primarily as the H_2 rate accelerated, and carbohydrate consumption preceding the H_2 production peak. Cellular glycogen concentrations at select time points were between 75 and 94% of the total carbohydrates, indicating that the observed dynamics were primarily a reflection of changes in glycogen.

Cessation of NH_4^+ influx was followed by a decline in total protein in both reactors as H_2 rates accelerated (Fig. 2c and d), followed by a recovery to the levels observed during steady state. From a biotechnological perspective, it is remarkable that prolonged N deprivation did not lead to a catastrophic decrease in protein content over the 100 h of the experiment. However, the accessory pigment phycocyanin had degraded to ~40% of the steady-state level over the first 24 h, with a further decline to ~20% after 50 h (see Fig. S3 in the supplemental material). In contrast, no substantial changes in the level of chlorophyll pigment could be observed.

Light dependence and photophysiology of H_2 production. *In situ* rates of O_2 and H_2 production were examined as a function of light intensity and quality (Fig. 3). At irradiances of <50 μmol m^{-2} s^{-1}, H_2 production was detectable, whereas net O_2 evolution was extremely low. The H_2 production rate reached saturation at irradiances lower than those at which O_2 evolution saturated and which were below the level of incident irradiance supplied to the bioreactor during feedback control (240 μmol m^{-2} s^{-1}). As O_2 evolution increased at higher irradiances, the H_2 production rates maintained the level achieved upon light saturation. Because the photobioreactor was irradiated with discrete LEDs that emitted at 630 or 680 nm, favoring either phycobilin or chlorophyll excitation, it was possible to measure light saturation curves for each pigment independently. At 680-nm ir-

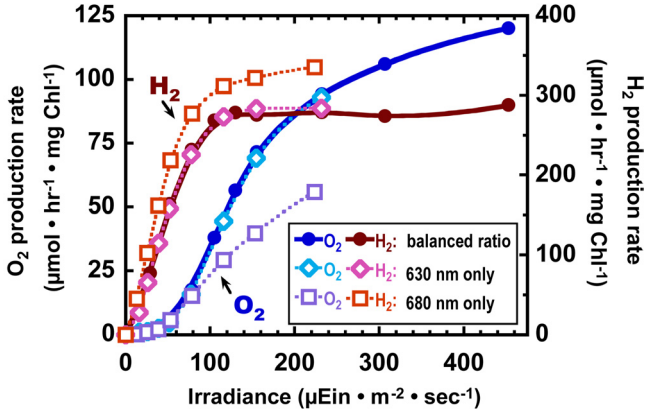

FIG 3 Light saturation of O_2 and H_2 production performed *in situ* within the photobioreactor. Experiments were performed after 16 h of CO_2-deprived H_2 production. Values represent the averages from two individual curves, performed 3 h apart.

radiance, the maximum rate of H_2 production was about 20% higher than when both wavelengths were presented, and the initial slope (alpha) was increased, representing enhanced light utilization efficiency of H_2 production (see Table S1 in the supplemental material). In contrast, photosynthetic production of O_2 had a much lower alpha when 680 nm of light was supplied alone, compared to the values with 630 nm alone or with a balanced profile. There does not seem to be an additive effect of supplying both wavelengths; furthermore, the inclusion of 630 nm light may slightly suppress the efficiency of H_2 production.

H_2 production activity was also measured in the presence of the electron transport inhibitors 3-(3,4-dichlorophenyl)-1,1-dimethylurea (DCMU) and p-benzoquinone (BQ) to investigate the dependence of the process upon photocatalytic H_2O oxidation (Fig. 4a and b). The specific PSII inhibitor, DCMU, completely and immediately inhibited PSII activity at concentrations as low as 1.0 μM (Fig. S4 in the supplemental material). As shown in Fig. 4a,

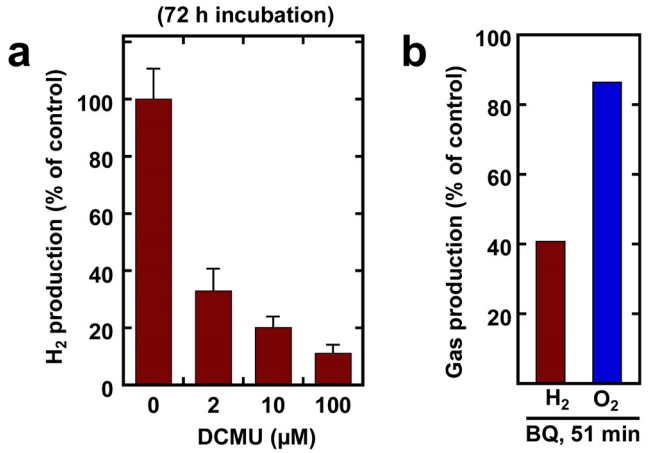

FIG 4 Effects of electron transport inhibitors in illuminated sealed tubes with an Ar atmosphere. (a) Incubation with DCMU for 72 h, using 10 ml chemostat cells. Control value (100%) was 3.28 mmol $H_2 \cdot mg\ Chl^{-1}$. (b) Treatment with p-benzoquinone (BQ) for 1 h, at 170 μM. Cells were sampled from a CO_2-deprived bioreactor, 78 h after NH_4^+ deprivation. Control values (100%, no BQ) were 34 and 346 $\mu mol \cdot mg\ Chl^{-1} \cdot h^{-1}$ for H_2 and O_2, respectively.

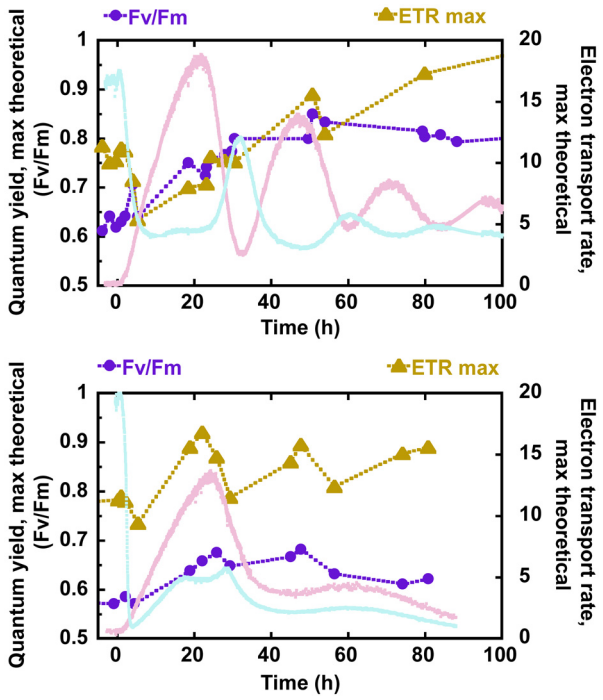

FIG 5 F_v/F_m and ETR_{max} during H_2 production for CO_2-supplied (a) and CO_2-deprived (b) reactor, as determined with PAM fluorometry.

long-term incubation with DCMU for 72 h caused a dramatic, but incomplete, inhibition of H_2 accumulation in the light. Remarkably, short-term (1-h) incubation of H_2-evolving cells did not inhibit H_2 production at any concentration (data not shown). The plastoquinone analog BQ was observed to cause a substantial inhibition of H_2 production after 50 min, with only a modest effect upon O_2 evolution (Fig. 4b).

The capacity for photosynthetic electron transport was further investigated by measuring the variable level of chlorophyll fluorescence originating from PSII, using a pulse amplitude modulated (PAM) fluorometer. The maximum theoretical quantum efficiency of PSII, represented by the proportion of the maximal fluorescence which varies according to PSII activity (F_v/F_m), showed an increase over the first 48 h of H_2 production in both bioreactors (Fig. 5). In the presence of CO_2, the F_v/F_m reached a higher value than that of the CO_2-deprived condition and maintained this high value throughout the second half of the experiment, whereas the F_v/F_m declined during the latter part of the CO_2-deprived experiment. Further information about PSII activity was obtained from rapid light curves using the saturating pulse method to infer the rate of linear electron transport from PSII. Under both reactor conditions, the maximal electron transport rate (ETR_{max}) showed a brief decline over the first few hours of nitrogen deprivation, thereafter rising concurrently with the H_2 production rate. However, in the CO_2-deprived condition, the ETR_{max} peaked at 22 h and subsequently oscillated between about 11 and 17 $\mu mol\ electrons \cdot m^{-2} \cdot s^{-1}$, whereas this parameter continued to rise further in the CO_2-supplied condition. It should be noted that, throughout the H_2 production process, neither of these photophysiological parameters decreased far below the starting values observed during steady-state growth, indicating a

robust capacity for photosynthesis during prolonged H_2 production over 100 h.

DISCUSSION

Future developments of H_2 as a photosynthetic biofuel depend on understanding how cells catalyze H_2 production concurrent with oxygenic photosynthesis (2). Here, we examined the photophysiological relationship between dinitrogenase-driven H_2 production and photosynthetic O_2 evolution and uncovered physiological conditions in which these processes co-occur. The experimental evidence revealed that metabolic dynamics and coordinated regulation of photosynthesis and dinitrogenase activity in *Cyanothece* 51142 displays oscillating patterns which may or may not be governed by circadian mechanisms or the onset of illumination during diurnal growth. Nonetheless, by avoiding the entrainment of cells to light-dark cycles—as no oscillations were observed during the NH_4^+-limited chemostat growth—such a mechanism is not necessary to precondition the cells for H_2 production. Irrespective of CO_2 supply, continuously illuminated N-deprived *Cyanothece* 51142 cells evolved H_2 at rates which accelerated steadily for 24 h. After 24 h, the H_2-producing cultures did begin to exhibit oscillations; however, only when CO_2 was available did the gas dynamics follow a pattern which resembled the 12-h alternating phases observed with entrained cultures; in stark contrast, there was a positive correlation between H_2 and O_2 evolution in the CO_2-deprived reactor, suggesting that not only was dinitrogenase activity protected from O_2 inactivation but it also alleviated photoinhibition. In fact, the dynamic measurements of biochemical and biophysical characteristics of H_2-producing *Cyanothece* 51142 reveal a lack of prominent photoinactivation (Fig. 3), stable chlorophyll levels (see Fig. S3 in the supplemental material), and robust electron transport capacity (Fig. 5). Despite the initial decline of PSII activity upon halting the delivery of NH_4^+, it appears that linear electron transport may recover and even be enhanced by the achievement of high rates of H_2 production. The correlated rise in O_2 and H_2 evolution rates during the first phase of the CO_2-deprived experiment (Fig. 1b) supports this hypothesis. Because there are few electron sinks under this condition, overreduction of the PQ pool leads to deleterious effects on PSII function (21); however, dinitrogenase-mediated proton reduction may provide relief (22) by consuming reductant and thus preventing PSII closure.

While the observation of concomitant O_2 and H_2 evolution in a well-mixed unicellular system is provocative from a photophysiology standpoint, it has important implications for biofuel production. Our results clearly demonstrate that these two activities proceeded uninterrupted for several days of continuous illumination. Although changes in rates of the two processes were phased, their co-occurrence persisted in the CO_2-supplied bioreactor. As dinitrogenase is primarily responsible for H_2 evolution (18), this research also suggests that the mechanism of aerotolerance has been underappreciated. While there is no reason to speculate that the protein itself is O_2 tolerant (23), the concept of "respiratory protection" (24) seems plausible, reminiscent of the situation in *Azotobacter* (25) and *Trichodesmium* (26). In *Cyanothece* 51142, such a mechanism is supported by the inflection in O_2 evolution coinciding with the appearance of CO_2 (Fig. 1a and b) as well as by the decline in carbohydrate content which begins whenever the H_2 rate approaches a maximum (Fig. 2a and b). Electron micrographs of diazotrophically grown *Cyanothece* 51142 had shown a homogenous distribution of immunogold-labeled dinitrogenase, suggesting a lack of physical separation from oxygenic photosynthesis (27); but this neither precludes the existence of intracellular O_2 gradients nor discounts the possibility that the enzyme may not be equally active throughout the cell.

Furthermore, continuous net O_2 evolution indicates that PSII activity was maintained throughout the experiment and raises the question of whether H_2O oxidation may directly contribute to H_2 production. The nearly immediate loss of detectable H_2 within 3 min of a shift to darkness underscores the importance of the photosynthetic light reactions (see Fig. S5 in the supplemental material). Although inactivation of PSII with the inhibitor DCMU had no short-term effect upon H_2 production, a dose-dependent inhibitory effect of DCMU was indeed observed upon prolonged incubation (Fig. 4a), suggesting that the provision of electrons from H_2O by PSII may be necessary to maintain the capacity for H_2 evolution. Furthermore, mass balance calculations indicate that the H_2O-derived electrons which must accompany the observed O_2 evolution are more than sufficient to account for the H_2 yield under Ar-only conditions (see Fig. S2c in the supplemental material).

The lack of any short-term inhibition by DCMU suggests a major role for PSI activity (26). The enhanced quantum efficiency of H_2 production with 680 nm compared to 630 nm light supports this (Fig. 3), especially as it coincided with a decreased efficiency of O_2 evolution, resembling the preferential excitation of PSI by chlorophyll-specific light. The inhibitory effect of BQ upon H_2 but not O_2 production (Fig. 4b) may further support the role of PSI, as this plastoquinone analog is known to oxidize the quinone pool, maintaining PSII function, although the downstream effects on electron transport are unclear. Similarly, important contributions by catabolism of endogenous organic carbon are also suggested by the correlated dynamics of H_2 and CO_2 evolution (Fig. 1a), the declining carbohydrate content which precedes maximal H_2 rates (Fig. 2a and b), and the requirement of exogenous O_2 for H_2 production in the dark (see Fig. S5 in the supplemental material). However, mass balance calculations using the stoichiometric H_2 yield of complete glucose oxidation suggest that carbohydrate consumption in the light may, at best, account for no more than 51% of the reductant required for the corresponding H_2 production (see Fig. S2 in the supplemental material), although this contribution may be much lower due to respiratory O_2 scavenging and/or the thermodynamic constraints of fermentative metabolism. Furthermore, under Ar-only conditions, significant H_2 production is still observed during the latter half of the experiment, when carbohydrate consumption is negligible.

These results imply that *Cyanothece* 51142 has a flexible metabolism in which different mechanisms and electron sources may be utilized for H_2 production (6, 12). The reductant and ATP necessary for H_2 production, as well as for cell maintenance, is likely supplied by linear electron transport through PSII and by light-independent substrate catabolism in the presence of O_2, with offsets in the demand for ATP fulfilled by cyclic electron transport around PSI. Moreover, as cyanobacterial thylakoid membranes have several branch points between photosynthetic and respiratory electron transport components (28), "pseudocyclic" processes involving both PSI and respiratory complexes may also contribute to the generation of reductant and ATP (29), as well as toward the minimization of oxidative photodamage (30). The observed oscillations may indeed involve regulatory phenomena

among these processes (28) but are likely also intertwined with feedback mechanisms at the level of the electron transport chain (31).

This work has a large significance for biotechnology: for the first time, unicellular phototrophs have been shown to produce H_2 and O_2 concomitantly without interruption for at least 100 h. The high rates of H_2 production attained with this strain of *Cyanothece* are in agreement with what had been previously cited as the highest yet reported for any oxygenic phototroph (18). Yet here, such substantial H_2 production rates were observable for an extended period, without requiring light-dark entrainment or high cell density. The sustainability of the process is highlighted by a lack of apparent photodamage and the dampening of oscillations toward the end of the CO_2-supplied experiment (Fig. 1a), which maintained significant rates of net H_2 and O_2 evolution with no clear sign of decay. Possibly, a fed-batch process with intermittent N replenishment might permit an improvement of the dampened rate, as was shown in purple bacteria (32). It is likely that the imposition of nitrogen limitation in a photobioreactor equipped with advanced process control was influential to these results, but such operation is more relevant to an industrial setting than most laboratory-scale batch experiments and is quite amenable to optimization. The continuous illumination should not be a practical concern, as indoor 24-h operation of bichromic LEDs, powered by electricity from advanced photovoltaics and other renewables, can permit large increases in solar utilization efficiency (33).

MATERIALS AND METHODS

Media and cultivation conditions. *Cyanothece* 51142 was routinely maintained in modified ASP-2 medium (34), containing 17 mM NH_4Cl, 0.03 mM $FeCl_3$, and 0.75 mM K_2HPO_4, under continuous white-light illumination (50 μmol m^{-2} s^{-1}) and air sparging. Controlled cultivation was carried out in BioFlo 3000 reactors (New Brunswick Scientific, Edison, NJ) using a 7.5-liter cylindrical borosilicate glass vessel housed within a custom-manufactured aluminum enclosure equipped with LED illuminator chips (Marubeni America Corp., New York, NY) and quantum sensors (LI-COR, Lincoln, NE). LEDs provided 630 and 680 nm of narrow-band light (20-nm half width), favoring phycobilin and chlorophyll absorbance, respectively. Feedback-controlled custom software (BioLume) maintained 5 μmol m^{-2} s^{-1} of transmitted light through the reactor for each wavelength. Incident irradiances were calibrated using a spherical quantum sensor (LI-COR). NH_4^+-limited chemostat cultures were established at a 5.5-liter working volume, 30°C, and pH 7.5 using modified low-N ASP-2 containing 0.75 mM NH_4Cl delivered at a 0.05 h^{-1} dilution rate and sparging with 1.3% CO_2-Ar gas mix (vol/vol) at 4.08 liters/min. Steady-state cultures maintained a stable optical density at 730 nm (OD_{730}) of 0.20, 4.5 μM dO_2, and incident irradiances of 40 and 73 μmol m^{-2} s^{-1} for 630- and 680-nm lights, respectively. The extractable chlorophyll level at steady state was determined to be 1.08 $\mu g \cdot ml^{-1}$. The total and the ash-free dry cell weights at steady state were measured as 181 and 79 $\mu g \cdot ml^{-1}$, respectively.

H_2 production experiments. *In situ* H_2 production was measured in bioreactors upon halting the medium and/or CO_2 influx while maintaining the other operating parameters. H_2 inhibition studies were carried out using NH_4-limited chemostat cells in sealed test tubes under Ar atmosphere. Unless noted, tubes were incubated for 72 h in an inverted position at 30°C under continuous white fluorescent lighting at 140 μmol m^{-2} s^{-1}. Endpoint measurements of gas accumulation were obtained by quenching biological activity with 200 microliters of 6 M HCl. Environmental effects were investigated by varying the initial gas composition or preinjection with stocks of the electron-transport inhibitors, 3-(3,4-dichlorophenyl)-1,1-dimethylurea and p-benzoquinone. Short-term effects were examined in H_2-producing cultures which were flushed with Ar immediately before incubation and analyzed without quenching.

Analytical procedures. Protein was quantified by the Lowry method after precipitation with trichloroacetic acid (35). Total carbohydrates and isolated glycogen (36) were measured using a modified phenol-sulfuric acid protocol (37). Chlorophyll was quantitated by 90% methanol extraction (38). Additionally, pigments were estimated from whole-cell absorbance spectra upon baseline correction with an exponential fit (39). Spectrophotometric measurements were done using Spectronic GeneSys 20 spectrophotometer (Thermo Scientific, West Palm Beach, FL) except when recording spectra with a BioSpec 1601 (Shimadzu, Columbia, MD).

In situ dissolved O_2 (dO_2) was measured with a polarographic sensor (InPro 6100 G, Mettler-Toledo Process Analytics), calibrated as 190 μM at air saturation (seawater, 30°C). *In situ* dissolved H_2 (dH_2) was measured with a modified O_2 sensor, which was adapted by reversing the polarity, preconditioning for 6 h in proprietary electrolyte (number 9920; Mettler-Toledo), swapping the electrolyte to an HCl/KCl solution (0.1 M each) (40), desensitizing with a certified gas mixture of 15,200 ppm H_2-Ar (American Air Liquide, Houston, TX), and calibrating as 11.53 μM (freshwater, 30°C). Instantaneous net production rates of H_2 and O_2 were obtained using first-order removal coefficients (74.320 and 55.024 h^{-1}, respectively), determined from the slope of the natural logarithm of dH_2 or dO_2 removal during brief darkness, averaged across six measurements. Bioreactor off-gas composition was measured by online mass spectrometry (MGA iSCAN, Hamilton Sunstrand). Gas composition of tube headspace was analyzed with a Hewlett-Packard 5890 series II gas chromatograph, using a thermal conductivity detector, Supelco 60/80 Carboxen 1000 column (Sigma-Aldrich, St. Louis, MO), and Ar carrier gas.

Photophysiological measurements. Light response curves for O_2 and H_2 evolution were determined *in situ* within the photobioreactor by interrupting BioLume's feedback control with a manual routine. Five-minute steps of increasing incident irradiance from each illuminator were implemented sequentially, following 10 min of darkness, and repeated with 630- or 680-nm LEDs independently. The average dO_2 or dH_2 at equilibrium for each step was converted to net production rate as described above and plotted against irradiance. Photosynthetic parameters were obtained by fitting the data to a hyperbolic tangent function (41). Variable chlorophyll fluorescence was measured using PAM fluorometry in a DUAL-PAM-100 system (Walz GmbH, Effeltrich, Germany) with a photodiode detector and RG665 filter (42). Red measuring light (620 nm) at the lowest power was pulsed at 1,000 Hz during the dark and at 10,000 Hz during 635-nm actinic illumination at 98 μmol m^{-2} s^{-1}. The maximum theoretical quantum yield of PSII (F_v/F_m) was calculated from maximal fluorescence (F_m-true) recorded with 15 μM DCMU during actinic illumination and minimal fluorescence (F_o) after 10 min of incubation with only far-red (730 nm) light (43). Electron transport rates through PSII were determined with rapid light curves (44) using 20-s steps of incremental actinic light followed by a 200-ms saturating pulse at 1,000 μmol m^{-2} s^{-1} and 5 s of only far-red light.

SUPPLEMENTAL MATERIAL

Supplemental material for this article may be found at http://mbio.asm.org/lookup/suppl/doi:10.1128/mBio.00197-12/-/DCSupplemental.

Figure S1, DOCX file, 0.1 MB.
Figure S2, DOCX file, 0.1 MB.
Figure S3, DOCX file, 0.1 MB.
Figure S4, DOCX file, 0.1 MB.
Figure S5, DOCX file, 0.1 MB.
Table S1, DOCX file, 0.1 MB.

ACKNOWLEDGMENTS

The research was supported by the Genomic Science Program (GSP), Office of Biological and Environmental Research (OBER), U.S. Department of Energy, and is a contribution of the PNNL Biofuels and Foundational Scientific Focus Areas (SFAs).

The authors acknowledge Jonathan Meuser for his help in developing

the dissolved H_2 electrode and Oleg Geydebrekht and Elizabeth Burrows for assistance with continuous cultivation and hydrogen production experiments. We are thankful to John Benemann, Michael Huesemann, and Blaine Metting for insightful discussions and general support throughout the project.

M.R.M., A.E.K., and A.S.B. conceptualized the research and wrote the manuscript. M.R.M. and L.A.K. planned and performed the experimentation, took samples, performed biochemical analyses, and calculated the data. G.E.P. and E.A.H. designed the photobioreactor and supervised reactor operations. M.R.M. and E.A.H. designed the dissolved hydrogen probe. E.A.H., G.E.P., J.K.F., and A.S.B. made the initial discovery of H_2 production and defined the chemostat operating parameters. A.S.B., A.E.K., and J.K.F. supervised the project. All authors edited the manuscript.

REFERENCES

1. **Romagnoli F, Blumberga D, Pilicka I.** 2011. Life cycle assessment of biohydrogen production in photosynthetic processes. Int. J. Hydrogen Energ. **36**:7866–7871.
2. **Ghirardi ML, Mohanty P.** 2010. Oxygenic hydrogen photoproduction—current status of the technology. Curr. Sci. **98**:499–507.
3. **McKinlay JB, Harwood CS.** 2010. Photobiological production of hydrogen gas as a biofuel. Curr. Opin. Biotechnol. **21**:244–251.
4. **Vignais PM, Billoud B.** 2007. Occurrence, classification, and biological function of hydrogenases: an overview. Chem. Rev. **107**:4206–4272.
5. **Ananyev G, Carrieri D, Dismukes GC.** 2008. Optimization of metabolic capacity and flux through environmental cues to maximize hydrogen production by the cyanobacterium "*Arthrospira* (*Spirulina*) *maxima*". Appl. Environ. Microbiol. **74**:6102–6113.
6. **Hemschemeier A, Fouchard S, Cournac L, Peltier G, Happe T.** 2008. Hydrogen production by *Chlamydomonas reinhardtii*: an elaborate interplay of electron sources and sinks. Planta **227**:397–407.
7. **Eroglu E, Melis A.** 2011. Photobiological hydrogen production: recent advances and state of the art. Bioresour. Technol. **102**:8403–8413.
8. **Bothe H, Schmitz O, Yates MG, Newton WE.** 2010. Nitrogen fixation and hydrogen metabolism in cyanobacteria. Microbiol. Mol. Biol. Rev. **74**:529–551.
9. **Gallon JR.** 1992. Reconciling the incompatible: N_2 fixation and O_2. New Phytol. **122**:571–609.
10. **Kumar K, Mella-Herrera RA, Golden JW.** 2010. Cyanobacterial heterocysts. Cold Spring Harbor Perspect. Biol. **2**:a000315.
11. **Zehr JP.** 2011. Nitrogen fixation by marine cyanobacteria. Trends Microbiol. **19**:162–173.
12. **Berman-Frank I, et al.** 2001. Segregation of nitrogen fixation and oxygenic photosynthesis in the marine cyanobacterium *Trichodesmium*. Science **294**:1534–1537.
13. **Compaoré J, Stal LJ.** 2010. Oxygen and the light-dark cycle of nitrogenase activity in two unicellular cyanobacteria. Environ. Microbiol. **12**:54–62.
14. **Sherman LA, Meunier P, Col MS.** 1998. Diurnal rhythms in metabolism: a day in the life of a unicellular, diazotrophic cyanobacterium. Photosynth. Res. **58**:25–42.
15. **Mitsui A, Suda S.** 1995. Alternative and cyclic appearance of H_2 and 0 2 photoproduction activities under non-growing conditions in an aerobic nitrogen-fixing unicellular cyanobacterium Synechococcus sp. Curr. Microbiol. **30**:1–6.
16. **Skizim NJ, Ananyev GM, Krishnan A, Dismukes GC.** 2012. Metabolic pathways for photobiological hydrogen production by nitrogenase-and hydrogenase-containing unicellular cyanobacteria *Cyanothece*. J. Biol. Chem. **287**:2777–2786.
17. **Wilson S, Foster R, Zehr J, Karl D.** 2010. Hydrogen production by *Trichodesmium erythraeum Cyanothece* sp. and *Crocosphaera watsonii*. Aquat. Microb. Ecol. **59**:197–206.
18. **Bandyopadhyay A, Stöckel J, Min H, Sherman LA, Pakrasi HB.** 2010. High rates of photobiological H_2 production by a cyanobacterium under aerobic conditions. Nat. Commun. **1**:139.
19. **Cervený J, Nedbal L.** 2009. Metabolic rhythms of the cyanobacterium *Cyanothece* sp. ATCC 51142 correlate with modeled dynamics of circadian clock. J. Biol. Rhythms **24**:295–303.
20. **Vu TT, et al.** 2012. Genome-scale modeling of light-driven reductant partitioning and carbon fluxes in diazotrophic unicellular cyanobacterium *Cyanothece* sp. ATCC 51142. PLoS Comput. Biol. **8**:e1002460.
21. **Collier JL, Herbert SK, Fork DC, Grossman AR.** 1994. Changes in the cyanobacterial photosynthetic apparatus during acclimation to macronutrient deprivation. Photosynth. Res. **42**:173–183.
22. **Joshi HM, Tabita FR.** 1996. A global two component signal transduction system that integrates the control of photosynthesis, carbon dioxide assimilation, and nitrogen fixation. Proc. Natl. Acad. Sci. U. S. A. **93**:14515–14520.
23. **Gallon JR, Pederson DM, Smith GD.** 1993. The effect of temperature on the sensitivity of nitrogenase to oxygen in the cyanobacteria *Anabaena cylindrica* (Lemmermann) and *Gloethece* (Nageli). New Phytol. **124**:251–257.
24. **Peschek GA, Villgrater K, Wastyn M.** 1991. "Respiratory protection" of the nitrogenase in dinitrogen-fixing cyanobacteria. Plant Soil **137**:17–24.
25. **Oelze J.** 2000. Respiratory protection of nitrogenase in *Azotobacter* species: is a widely held hypothesis unequivocally supported by experimental evidence? FEMS Microbiol. Rev. **24**:321–333.
26. **Milligan AJ, Berman-Frank I, Gerchman Y, Dismukes GC, Falkowski PG.** 2007. Light-dependent oxygen consumption in nitrogen-fixing cyanobacteria plays a key role in nitrogenase protection. J. Phycol. **43**:845–852.
27. **Colón-López MS, Sherman DM, Sherman LA.** 1997. Transcriptional and translational regulation of nitrogenase in light-dark- and continuous-light-grown cultures of the unicellular cyanobacterium *Cyanothece* sp. strain ATCC 51142. J. Bacteriol. **179**:4319–4327.
28. **Peschek GA, Obinger C, Paumann M.** 2004. The respiratory chain of blue-green algae (cyanobacteria). Physiol. Plant. **120**:358–369.
29. **Allen JF.** 2003. Cyclic, pseudocyclic and noncyclic photophosphorylation: new links in the chain. Trends Plant Sci. **8**:15–19.
30. **Niyogi KK.** 2000. Safety valves for photosynthesis. Curr. Opin. Plant Biol. **3**:455–460.
31. **Trubitsin BV, et al.** 2005. EPR study of electron transport in the cyanobacterium Synechocystis sp. PCC 6803: oxygen-dependent interrelations between photosynthetic and respiratory electron transport chains. Biochim. Biophys. Acta. **1708**:238–249.
32. **Melnicki M, Bianchi L, Dephilippis R, Melis A.** 2008. Hydrogen production during stationary phase in purple photosynthetic bacteria. Int. J. Hydrogen Energ. **33**:6525–6534.
33. **Gordon JM, Polle JEW.** 2007. Ultrahigh bioproductivity from algae. Appl. Microbiol. Biotechnol. **76**:969–975.
34. **Van Baalen C.** 1962. Studies on marine blue-green algae. Bot. Mar. **4**:129–139.
35. **Melnicki MR, Eroglu E, Melis A.** 2009. Changes in hydrogen production and polymer accumulation upon sulfur-deprivation in purple photosynthetic bacteria. Int. J. Hydrogen Energ. **34**:6157–6170.
36. **Del Don C, Hanselmann KW, Peduzzi R, Bachofen R.** 1994. Biomass composition and methods for the determination of metabolic reserve polymers in phototrophic sulfur bacteria. Aquat. Sci. **56**:1–15.
37. **Cuesta G, Suarez N, Bessio MI, Ferreira F, Massaldi H.** 2003. Quantitative determination of pneumococcal capsular polysaccharide serotype 14 using a modification of phenol-sulfuric acid method. J. Microbiol. Methods **52**:69–73.
38. **Meeks JC, Castenholz RW.** 1971. Growth and photosynthesis in an extreme thermophile, *Synechococcus lividus* (Cyanophyta). Arch. Mikrobiol. **78**:25–41.
39. **Burns RA, Mac Kenzie TDB, Campbell DA.** 2006. Inorganic carbon repletion constrains steady-state light acclimation in the cyanobacterium *Synechococcus elongatus*. J. Phycol. **42**:610–621.
40. **Kuroda K, Gaigersilveira R, Nishio N, Sunahara H, Nagai S.** 1991. Measurement of dissolved hydrogen in an anaerobic digestion process by a membrane-covered electrode. J. Ferment. Bioeng. **71**:418–423.
41. **Jassby AD, Platt T.** 1976. Mathematical formulation of the relationship photosynthesis and light for phytoplankton. Mar. Ecol. **21**:540–547.
42. **Schreiber U.** 1986. Detection of rapid induction kinetics with a new type of high-frequency modulated chlorophyll fluorometer. Photosynth. Res. **9**:261–272.
43. **Campbell D, Hurry V, Clarke AK, Gustafsson P, Oquist G.** 1998. Chlorophyll fluorescence analysis of cyanobacterial photosynthesis and acclimation. Microbiol. Mol. Biol. Rev. **62**:667–683.
44. **White AJ, Critchley C.** 1999. Rapid light curves: a new fluorescence method to assess the state of the photosynthetic apparatus. Photosynth. Res. **59**:63–72.